The influence of abruptly variable cross-section on oil core eccentricity and flow characteristics during viscous oil-water horizontal flow

P. Babakhani Dehkordi [a*], L.P.M. Colombo [a], E. Mohammadian [b,c*], A. Azdarpour [d], G. Sotgia[a]

a: Politecnico di Milano, Department of Energy, via Lambruschini 4, 20156 Milan, Italy

b: Department of Management of Science and Technology Development, Ton Duc Thang University, Ho Chi Minh City, Vietnam

c: Faculty of Applied Sciences, Ton Duc Thang University, Ho Chi Minh City, Vietnam

d: Department of Petroleum Engineering, Marvdasht Branch, Islamic Azad University, Marvdasht, Iran

Corresponding author*: Parham Babakhani Dehkordi (Babakhani65@gmail.com)

Co-corresponding author*: Erfan Mohammadian (erfan.mohammadian@tdtu.edu.vn)

1. Introduction

Design of pipeline downstream of hydrocarbon wells is highly dependent upon topology of region where oil is flowing. Thus, frequent area changes in pipeline systems such as expansions, contractions, existence of risers, valves, and elbows, etc. are present. In the last decades (beginning with development of nuclear plants), there have been a large number of research studies on two-phase gas-liquid flows in the presence of singularities, e.g. sudden contraction and expansion, see for instance, Wadle (1989), Attou and Bolle (1997), Chen et al. (2007) and Chen et al. (2009). However, a complete and general characterization of the fluid dynamics downstream the geometric singularity is far from being achieved.

One of the useful approaches to transport heavy oil in pipeline is the so-called water-lubricated flow, which enables significant saving in pumping power by establishing core-annular flow. In this flow pattern, the oil core is encircled by a less viscous water annulus, leading to considerable decrease in the frictional pressure drop, which may lower to values almost comparable to the single-phase water flow. The vast majority of the related published work deals with viscous oil-water mixture within straight horizontal pipelines. During the past years, we can mention the works by Charles et al. (1961), Ooms et al. (1984), Oliemans et al. (1987), Arney et al. (1993), Bannwart et al. (2004), Grassi et al. (2008), Sotgia et al. (2008), Colombo et al. (2012).

Recently, experiments on very viscous oil (oil viscosity ranged from 3.3 to 16.0 Pa·s) and water flows were conducted in a horizontal 25.4 mm i.d. pipe by Shi (2015). Superficial oil velocity was in the range 0.04-0.54 m/s, while water superficial velocity was varied between 0.01-1.8 m/s. Different flow patterns were observed, which included oil-continuous (OC), phase inversion (Inv), core-annular flow (CAF), oil plugs in water (OPL), dispersed oil lumps in water (OLP). Pressure drop and holdup were measured by means of sampling method. The results were compared to the CFD analyses under different operating conditions. It was found that the relative errors between predicted pressure drop and measurements could grow up to 69%. In particular, CFD failed in predicting the pressure drop in the operating conditions characterized by contact of a thin layer of oil with the wall, as documented by flow visualizations. On the other hand, the water holdup calculated from CFD simulation showed satisfactory agreements with experimental Quick Closing Valve (QCV) data.

The work by Loh and Premanadhan (2016) dealt with oil-water flows within a 27.86 mm i.d. pipe. Two different oils were used: light oil (μ_o=0.030 Pa·s) and heavy oil (μ_o=0.3 Pa·s). Distributed pressure drops were measured and reported as a function of the oil holdup and superficial mixture velocity. They concluded that pressure drop for light oil has is lower than that of heavy oil, which was associated with higher shear stresses between viscous oil and wall. In addition, they found discrepancies between flow patterns of light and heavy oils, i.e., the domain of existence of dispersed oil in water flow pattern was significantly reduced in the latter case.

Van Duin et al. (2018) investigated oil-water core-annular flow within a 21 mm i.d. pipe, with focus on the effects of oil viscosity on pressure drop. Oil viscosity varied from 0.35 Pa·s at 20 °C to 2.7 Pa·s at 50 °C. The ratio between two-phase and only oil pressure drop was reported as a function of oil viscosity. The main conclusion was that at higher oil viscosity the scaled pressure drop is independent of the input volumetric water fraction. Furthermore, flow visualization showed that smaller wavelength with irregular shape was observed at the oil-water interface by reducing oil viscosity.

As far as liquid-liquid flow through singularities is concerned, a limited number of research activities have been published, in spite of the relevance to petroleum industry. One may refer to the works carried out by Hwang and Pal (1997), Balakhrisna et al. (2010), Kaushik et al. (2012), Colombo et al. (2015), Babakhani et al. (2017, 2017b, 2018).

Hwang and Pal (1997) measured pressure losses for oil-in-water and water-in-oil emulsions through sudden expansions (from 20.37 mm to 41.24 mm i.d.) and contractions (from 41.24 mm to 20.37 mm i.d). Oil viscosity varied from 0.9 mPa·s to 13.90 mPa·s depending on the temperature. The concentrated pressure drop was obtained by extrapolation of the distributed pressure gradients downstream and upstream of the singularity (i.e. the section of abrupt change in the flow area). Based on measured concentrated pressure drop the values of loss coefficients were reported as a function of oil concentration. It was concluded that the loss coefficient is not considerably affected by the type and concentrations of emulsions.

Balakhrisna et al. (2010) performed experimental tests for oil-water mixture within ducts undergoing abrupt expansion from 12 mm to 25 mm and abrupt contraction from 25 mm to 12 mm, considering lube oil (μ_o=0.2 Pa·s and ρ_o=960 kg·m^{-3}) and kerosene (μ_o=0.0012 Pa·s and ρ_o=787 kg·m^{-3}). Change of spatial distribution of phases downstream of the singularity was investigated. They concluded that sudden expansion caused thickening of oil core for lube oil in the downstream pipe. As a result, the stability of core-annular flow is increased. On the contrary, care must be taken downstream of a sudden expansion where the oil core is thicker and more eccentric, with increased probability of contacting the wall. . Loss coefficients were measured and found comparable to the values obtained by Hwang and Pal (1997).

Colombo et al. (2015) studied viscous oil-water flow in a horizontal pipe with sudden contractions from 50 mm to 30 mm i.d. and from 50 mm to 40 mm i.d. Accordingly, contraction ratios (ratio between smaller to larger pipe diameters) were ς=0.36 and ς=0.64, respectively. Mineral oil (μ_o=0.838 Pa·s at 20 °C; ρ_o=890 kg·m^{-3}) and tap water were used. In situ oil fraction (holdup) was determined by means of sampling method in which two ball valves were used to instantaneously trap oil-water mixture. This shut-in system was positioned at a distance of 2.5 m from contraction plane. The results of oil holdup were compared to Arney et al. (1993) empirical correlation, showing an excellent agreement: maximum relative error was 5.15% for ς=0.64 and 5.88% for ς=0.36.

The work by Babakhani et al. (2017b) may also be cited, dealing with application of image processing technique to quantify viscous oil-water flow through a sudden expansion from 30 mm to 50 mm i.d. The same oil as in the work of Colombo et al. (2015) was used. The flow under investigation was dispersed oil drops in continuous water flow. Axial and radial velocity profiles, and holdup at the locations downstream very close to the singularity were analyzed. It was found that the developing length is dependent on the oil input volume fraction, that is, at higher input oil volume fraction the flow became fully developed at axial distance of L/D=4. This distance increased when oil volume fraction was reduced. It was experimentally observed that oil drops tended to migrate to the upper parts of duct with water always present at the pipe wall.

Some authors attempted to perform three-dimensional numerical simulations of the liquid-liquid flow across geometrical singularities. Kaushik et al. (2012) used the Volume of Fluid (VOF) approach to assess the influence of sudden expansions and contractions on phase holdup and pressure gradient. Numerical results were validated by the experimental data of Balakhrisna et al. (2010), indicating satisfactory agreement. The hydrodynamic behavior of viscous oil-water mixture through Venturi and Nozzle flow meters, and sudden expansions has been recently studied by Babakhani et al. (2017, 2018), respectively, who used VOF model to predict pressure gradient, phase holdup, and flow regime downstream of the singularity. The main flow regimes included core-annular flow (CAF), transition from CAF to dispersed flow, and dispersed flow. According to their findings, the expansion forced the oil core to be more eccentric with a thin layer of water between top of oil core and the pipe wall. In addition, both investigations confirmed that Computational Fluid Dynamic (CFD) approaches are unable to capture the dispersion of oil drops in continuous water flow, which would require extremely fine mesh. A summary of experimental studies on oil-water flows undergoing sudden expansions and contractions is listed in Table 1.

Empirical correlations and mechanistic models are useful methods to predict the design parameters of two-phase pipelines, even if they cannot provide comprehensive details about the local distribution of the major quantities. As far as liquid-liquid flows are concerned, a certain number of models dealing with core annular flow in horizontal pipes have been presented in the literature. Among them, the empirical correlations of Arney et al. (1993), Oliemans et al. (1987) and the mechanistic models of Brauner (1998), Ullmann and Brauner (2004), Colombo et al. (2017) for oil-water flow can be cited. The basic theory underlying these models, however, assumed axis-symmetric flow of oil-water mixture and did not consider explicitly the influence of core eccentricity. However, it was experimentally observed that core eccentricity is severe, particularly downstream of sudden expansions. Application of such models has been validated for pipe diameters lower than 40 mm (see e.g. Sotgia et al, 2008 and Shi et al, 2017). Accordingly, the present paper aims at evaluating the applicability of these models to larger pipe diameters downstream of sudden expansions where core eccentricity is dominant. Furthermore, a new expression to estimate oil holdup is proposed to include the effect of oil core eccentricity. Such a model has been validated against experimental data suitably collected in a dedicated test rig and added to the findings of Charles et al. (1961), Colombo et al. (2015), Shi et al. (2017). The results have been also compared with the other available models in the open literature. It is shown that the proposed model for oil holdup improves the prediction of the distributed pressure drop for eccentric core flows. Eventually, the concentrated pressure drop at the geometrical singularity has been estimated by means of pressure gradient extrapolation, which has enabled evaluation of the localized loss coefficients only available at present for low viscosity oil-water mixtures (see e.g. Hwang and Pal, 1997 and Balakhrisna et al, 2010). The paper is organized as follows. The available empirical and mechanistic models for liquid-liquid (oil-water) core annular flow are first described in section 2. Then, experimental facility and procedure are explained in section 3, followed by experimental results and evaluation of models in section 4. Conclusions are drawn in section 5.

Table 1 Summary of experimental investigations on oil-water flows through singularity

Author	Pipe configuration	ς (-)	ρ_o (kg/m^3)	μ_o (Pa.s)	Velocity (m/s)	Observed flow pattern[(a)]	Experimental measurement
Hwang and Pal (1997)	Sudden expansion & contraction	0.24	780	0.0027	Not reported	Emulsion (w/o) and (o/w)	Concentrated pressure drop, loss coefficient
Balakhrisna et al. (2010)	Sudden expansion & contraction	0.23	787 960	0.0012 0.2	J_o & J_w Up to 2.5	Thick, thin, sinuous core, oil dispersed, plug flow	Concentrated pressure drop, loss coefficient
Colombo et al. (2015)	Sudden contraction	0.36 0.64	890	0.838	J_o:0.43-1.48 J_w:0.34-2.37	D, EAD, EA, S	Holdup
Babakhani et al. (2017b)	Sudden expansion	0.36	890	0.838	J_o:0.29-0.59 J_w:0.56-0.84	Dispersed flow	Velocity profile, Holdup

(a) The nomenclature used in the work by Colombo et al. (2015) regarding flow patterns includes: D) dispersed flow, EAD) eccentric annular with big drops, EA) eccentric annular, S) stratified (oil contact at the wall)

2. Phenomenological and mechanistic models for core annular flow.

2.1 Oliemans et al. (1987)

An empirical correlation was developed by Oliemans (1987) in which water holdup measured by photographs was correlated to input water volume fraction as:

$$H_w = \varepsilon_w[1 + 0.2(1 - \varepsilon_w)^5] \quad (1)$$

This correlation was developed, considering a very viscous oil (μ_o=3.0 Pa·s) in a duct of 51 mm i.d.

2.2 Arney et al. (1993)

A simple empirical correlation to predict water holdup was proposed by Arney et al. (1993).

$$H_w = \varepsilon_w[1 + C\ (1 - \varepsilon_w)] \quad (2)$$

Where C=0.35. The water holdup is expressed in terms of input water volume fraction and it is similar to the correlation developed by Oliemans (1987). They used a broader experimental database to predict water holdup. Furthermore, Arney et al. (1993) considered perfect liquid-liquid core-annular flow and applied the Navier-Stokes equation to relate pressure gradient to total flow rate. A two-phase flow characteristic Reynolds number was defined for core-annular flow as a function of rheological properties of phases, pipe diameter, water-holdup, and mixture superficial velocity, such as:

$$Re_A = \frac{\rho_c D\ J_m}{\mu_w}\ [1 + \eta^4(\frac{\mu_w}{\mu_o} - 1)] \quad (3)$$

$$\eta = \sqrt{1 - H_w} \quad (4)$$

$$\rho_c = (1 - H_w)\rho_o + H_w\rho_w \quad (5)$$

To compute the characteristic two-phase Reynolds number from Equation (3), information of water holdup is required, which is calculated from Equation (2).

Arney et al. (1993) also predicted the pressure gradient following the Darcy-Weisbach equation as:

$$-\frac{dp}{dx} = \frac{f}{D}\frac{\rho_c J_m^2}{2} \qquad (6)$$

Where, f is the friction factor for the perfect core-annular flow and is expressed for laminar flow as:

$$f = \frac{64}{Re_A} \qquad (7)$$

For turbulent flow, the Blasius formulation was used, therefore:

$$f = 0.316\, {Re_A}^{-0.25} \qquad (8)$$

Notice that equation (7) and (8) are the conventional expressions of the friction factor as used for single-phase flow, owing to the special definition of Re_A.

2.3 Brauner (1998)

Brauner (1998) developed a mechanistic model based on the two-fluid approach for two immiscible fluids, denoted in the following with subscripts w and o, in a horizontal or slightly inclined duct. By assuming fully developed flow, the integral forms of the momentum equations for the water (w) in the annular domain and oil (o) in the core can be written as:

$$-A_w \frac{dp}{dx} - \tau_w S_w + \tau_i S_i + \rho_w\, A_w\, g\, \sin\beta = 0 \qquad (9)$$

$$-A_o \frac{dp}{dx} - \tau_i S_i + \rho_o\, A_o\, g\, \sin\beta = 0 \qquad (10)$$

In the above equations, A_w, and A_o are the actual areas occupied by water and oil, respectively. Here, pure oil phase and pure water phase, without entrainment of one phase into another are assumed. Eliminating the pressure gradient terms, it yields:

$$-\tau_w \frac{S_w}{A_w} \pm \tau_i S_i \left(\frac{1}{A_o} + \frac{1}{A_w}\right) + (\rho_w - \rho_o)\, g\, \sin\beta = 0 \qquad (11)$$

It is worth noting that the last term in Eq. 11 vanishes in the case of horizontal pipe. Brauner (1998) provided the simple explicit solutions for the in-situ holdup and dimensionless pressure gradient for the case of laminar oil (see Brauner, 1998 for more details). In a more recent work, Ullmann and Brauner (2004) provided an analytical solution of the two-fluid model, suggesting an improved correlation for the interfacial shear stress.

2.4 Colombo et al. (2017)

Colombo et al. (2017) predicted the holdup and pressure drop based on the two-fluid model. However, differently from Brauner (1998) the terms related to the interfacial shear stress was eliminated, and the holdup value has been directly determined from the measured pressure drop. The advantage of this method relies on the fact that it is much simpler to measure pressure drop rather than holdup, and in many industrial applications, the latter cannot be measured at all. The water holdup as a function of the superficial velocity and the measured pressure gradient is:

$$H_w = \left[\frac{C_w \left(\frac{\rho_w J_w D}{\mu_w} \right)^{-n_w} \rho_w {J_w}^2}{\left(-\frac{dp}{dx} \right) \frac{D}{2}} \right]^{0.5} \qquad (12)$$

For the laminar flow regime C_w=16 and n_w=1, whereas for developed turbulent flows, the Blasius formulation is often used; accordingly, C_w=0.079 and n_w=0.25 and for Re < 50000. C_w=0.046 and n_w=0.2 for Re > 50000. The value of water holdup was estimated based on eq. 12, considering measured pressure drop for oil-water mixture through horizontal pipe with D=21 mm, D=30 mm, D=40 mm. From Least square fitting on a very large database, the value of C=0.36 in Arney et al. (1993) correlation is obtained without significant difference. Of course, equation 12 can be rearranged to predict two-phase pressure drop once the holdup is known:

$$-\frac{dp}{dx} = 2C_w\left(\frac{\rho_w J_w D}{\mu_w}\right)^{-n_w}\frac{\rho_w J_w^2}{DH_w^2} \quad (13)$$

The summary of above models is presented in Table 2.

Table 2 Water holdup and pressure gradient for Laminar oil-Turbulent annular flow[(a)]

Author	Model	Additional information

Oliemans et al. (1987)	$H_w = \varepsilon_w[1 + 0.2(1 - \varepsilon_w)^5]$	$\varepsilon_w = J_w/J_m$ $J_m = J_w + J_o$
Arney et al. (1993)	$H_w = \varepsilon_w[1 + 0.35\ (1 - \varepsilon_w)]$	$\varepsilon_w = J_w/J_m$
Brauner (1998)	$H_w = 1 - \left(\frac{\phi}{(\phi X) + \phi + 1}\right)$ $\phi_A = \frac{K_1}{\phi}\left[\frac{(K_1\phi)^{0.5} + \phi + 1}{(K_1\phi)^{0.5} + 1}\right]^2$ $-\left(\frac{dp}{dx}\right) = \phi_A\left[\left(\frac{4C_c}{D}\right)\left(\frac{\rho_o J_o D}{\mu_o}\right)^{n_c}\left(\frac{\rho_o J_o^2}{2}\right)\right]$	$\phi = J_o/J_w$ $K_1 = \frac{0.046}{16}\frac{\mu_w}{\mu_o}Re_{ws}^{0.8}$ $X^2 = \frac{0.046}{16}\frac{\mu_w}{\mu_o}\frac{1}{\phi}Re_{ws}^{0.8}$
Ullmann and Brauner (2004)	$H_w = \frac{c_i^0/2 - X^2\,\phi/F_i + \frac{c_i^0}{2}\left[1 + 4X^2\left(\frac{\phi}{c_i^0}\right)^2\right]^{0.5}}{c_i^0 + \phi - X^2\,\phi/F_i}$	$c_i^0 = 1.17, F_i = 1$
Colombo et al. (2017)	$H_w = \left[\frac{C_w\left(\frac{\rho_w J_w D}{\mu_w}\right)^{-n_w}\rho_w {J_w}^2}{\left(-\frac{dp}{dx}\right)\frac{D}{2}}\right]^{0.5}$ or $H_w = \varepsilon_w[1 + 0.36\ (1 - \varepsilon_w)]$ $-\frac{dp}{dx} = 2C_w\left(\frac{\rho_w J_w D}{\mu_w}\right)^{-n_w}\frac{\rho_w J_w^2}{DH_w^2}$	C_w=0.079 and n_w=0.25 for Re < 50000 C_w=0.046 and n_w=0.2 for Re > 50000

(a) Prediction of pressure drop by Arney et al. (1993) empirical model is introduced in the text.

3. Experiments

3.1 Experimental setup and procedure

The experimental facility is depicted in Fig. 1 with sudden expansion as a test section downstream of inlet injector devices. Sudden contraction with the same pipe length was installed after measuring pressure drop concerning sudden expansion cases. The following configurations were then tested: one sudden contraction (TS1: 30-21 mm with ς=0.49) and three sudden expansions (TS2: 21-30 mm with ς=0.49, TS3: 30-40 mm with ς=0.56, TS4: 30-50 mm with ς=0.36). The horizontal pipeline is composed of 12 m transparent Plexiglass (to visualize flow pattern) where flow area change occurs 7 m from the inlet mixing device. The rheological properties of mineral oil and tap water are reported in Table 3. A specially designed mixing-device is adopted in the present study where water is injected peripherally by using a pipe, located with inclination angle of 25° with respect to the horizontal axis, and oil is introduced axially in order to promote the onset of core-annular flow regime. Pressure taps are installed at regular distances both at upstream and downstream of the geometrical singularity to measure the pressure drops. The pipes composing the test section are connected by flanges. The pressure taps are installed through small holes drilled in the pipe wall (i.d. 2-3 mm) and connected by small Nylon tubes to a differential pressure transducer (the choice of it depends on the pipe diameter with full scales ranging from 6.89 kPa to 68.9 kPa and full span accuracy of ±0.25%). Such an arrangement enables evaluating the pressure variation along the pipe both upstream and downstream of the flow area change. The water and oil volumetric flow rates are measured by means of magnetic flow meter (with a measureable range of 0.5-6.0 m^3/h and accuracy ±0.5 % of the reading) and adjustable metering gear pump, respectively. The two phases are separated in a 1 m^3 tank at the end of the pipeline, and then drawn to their respective storage tanks.

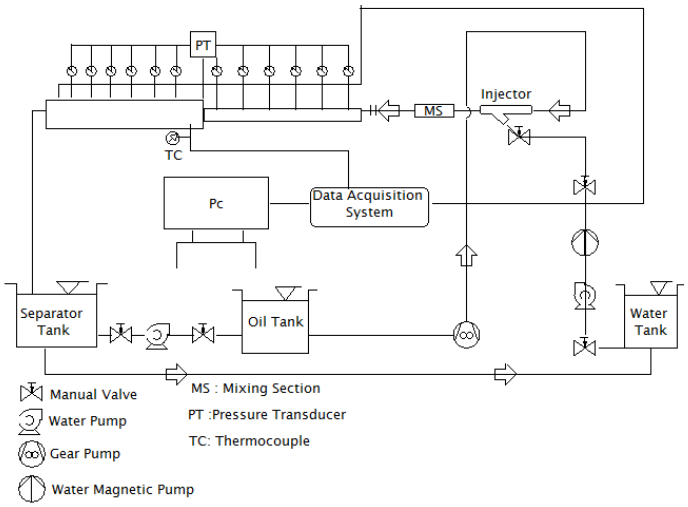

Fig.1 Sketch of experimental setup

Table 3 Physical properties of test fluids

Test fluids	ρ (kg/m^3)	μ (Pa·s)	σ (N/m)	$\sigma_{o\text{-}w}$ (N/m)
Oil Milpar 220	890	838×10^{-3}	0.035	0.02
Tap water	998	1.02×10^{-3}	0.073	

During experimental runs, water is introduced to the test section at the maximum volumetric flow rate to properly wash and fill the duct. Then, oil is injected at the selected superficial oil velocity (J_o), and the superficial water velocity is set to the desired value at each run. After segregation of the phases, a new test is performed by changing the superficial oil velocity. A digital HD video camera recorder (Nikon model D90) with frequency 50 fps was used to visualize flow patterns both upstream and downstream of the flow area change. Table 4 shows a summary of operating conditions considered in the current study.

Table 4 Summary of experimental runs for measurement of pressure drop

D (mm)	J_o (m/s)	J_w (m/s)	Re_{so} (m/s)	Re_{sw} (m/s)

21	1.67	0.49-0.74	37	10269-15509
	2.23	0.49-0.74	49	10269-15509
	2.79	0.36-0.63	62	7545-13203
	3.35	0.32-0.59	75	6706-12365
30	0.81	1.18-2.34	26	35329-70060
	1.09	1.18-2.34	35	35329-70060
	1.37	1.18-2.34	44	35329-70060
	1.64	1.18-2.34	52	35329-70060
40	0.46	0.67-1.34	19	26746-53493
	0.53	0.67-1.34	22	26746-53493
	0.61	0.67-1.34	25	26746-53493
	0.69	0.67-1.34	29	26746-53493
	0.77	0.67-1.34	33	26746-53493
	0.84	0.67-1.34	36	26746-53493
	0.92	0.67-1.34	39	26746-53493
50	0.29	0.42-0.85	15	20958-42415
	0.39	0.42-0.85	21	20958-42415
	0.49	0.42-0.85	26	20958-42415
	0.59	0.42-0.85	31	20958-42415

4. Results and discussions

4.1 Flow patterns

The focus of the present study is to characterize core-annular flows, hence, stratified flow regime is not considered, though in some operating conditions, transition from core-annular to stratified wavy flow or from core-annular to dispersed flow were detected. Visual observation is useful to evaluate the effect of flow disturbances in the downstream pipe caused by the sudden change in cross-sectional area. The following flow patterns can be classified.

Dispersed oil-in-water flow (D). At sufficiently high superficial velocity of water, dispersion of oil drops within continuous water flow occurs. The degree of dispersion is highly dependent on the oil flow rate. At the higher oil flow rates oil drops tend to collide together. On the other hand, increasing water superficial velocity would result in breaking oil drops into smaller ones, which is supposedly due to increased turbulent shear stress.

Core-annular flow (CAF). Core-annular flow regime is a flow regime observed in a wide range of superficial velocities for very viscous oil-water flows. It is the most frequently observed flow regime in the current study. The lower bound is reached by reducing the oil flow rate at constant water flow rate and vice versa. A particular type of CAF is the so-called Concentric CAF, where the oil core is nearly symmetric about the pipe axis.

Eccentric core-annular (ECA): Eccentric core-annular flow is a type of core-annular flow where the oil core tends to migrate to the upper part of pipe due to the effect of buoyancy. In the present study, two variations have been observed: a) Eccentric core-annular with oil drop entrainment (ECA-E) at the fluids interface , and b) Eccentric core-annular without oil drop entrainment (ECA) where no oil entrainment is observed at the oil-water interface.

Corrugated core-annular flow (CCA). This is a type of core-annular flow characterized by a very thin water layer adjoining the wall and an almost concentric oil core.

The photographic images of flow downstream of the sudden expansion for the minimum and maximum J_o and J_w are reported in Table 5 to show the flow evolution. Frames are taken at a location less than 10 diameters from the singularity to evaluate the distortion caused by the cross-section area change on the flow patterns. It is worth remarking that similar input volume flow rates are considered for all the cases of sudden expansions (TS2, TS3, and TS4). It is observed that the major disturbance consists of an increased entrainment rate at the oil-water interface. However, the dominant flow regime remains core-annular flow, mainly eccentric. As the water superficial velocity increases, the flow patterns gradually evolve to disperse patterns of oil drops, as a result of the increasing entrainment rate, which depends in turn on the higher interfacial shear stress. The oil core tends to remain concentric in the case 21-30 mm, while eccentricity is increased in the cases 30-40 mm and 30-50 mm.

Table 5 Flow pattern for downstream of sudden expansion (flow direction is from right to left)

Pipe configuration	J_o ($m \cdot s^{-1}$)	J_w ($m \cdot s^{-1}$)	Flow pattern
TS2: 21-30 mm	2.23	2.40	
	2.23	2.80	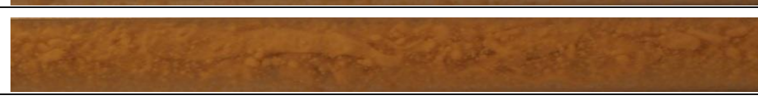
	3.35	2.40	
	3.35	2.80	

TS3: 30-40 mm	1.09	1.17	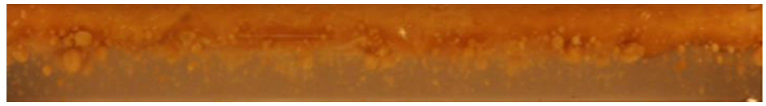
	1.09	1.37	
	1.64	1.17	
	1.64	1.37	
TS4: 30-50 mm	1.09	1.17	
	1.09	1.37	
	1.64	1.17	
	1.64	1.37	

4.1.1 Flow pattern maps

Flow pattern maps relative to the flow downstream of sudden expansions 21-30 mm (Fig. 2-a), 30-40 mm (Fig. 2-b), 30-50 mm (Fig. 2-c) are presented. For 21-30 mm and 30-40 mm, the dominant flow pattern is CAF, while for sudden expansion 30-50 mm, the main flow pattern is dispersed flow. Regarding the type of CAF flow regime, it is evident that concentric CAF is only present in the case of 21-30 mm, however, eccentricity plays an important role in the other ones.

According to operating conditions under investigations, CCA is only observed in the case of abrupt expansion from 30-40 mm. The boundaries between different flow regimes are indicated according to flow visualizations. In particular, the transition between stratified and dispersed flow is observed only for the case 30-50 mm (Fig. 2-c). In the other cases only transition between core-annular and dispersed flow is observed.

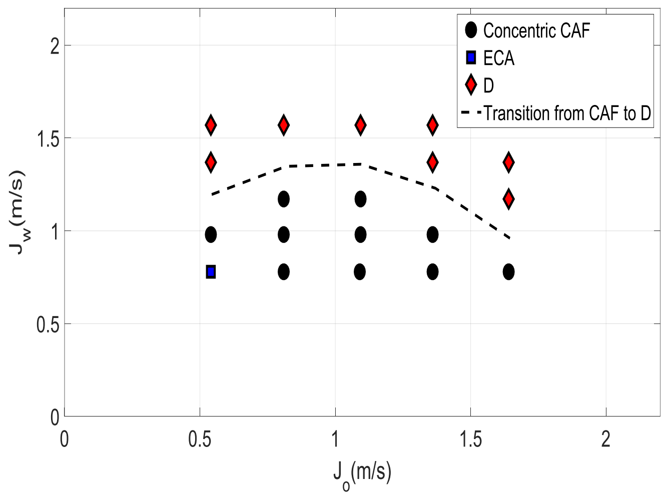

(a)

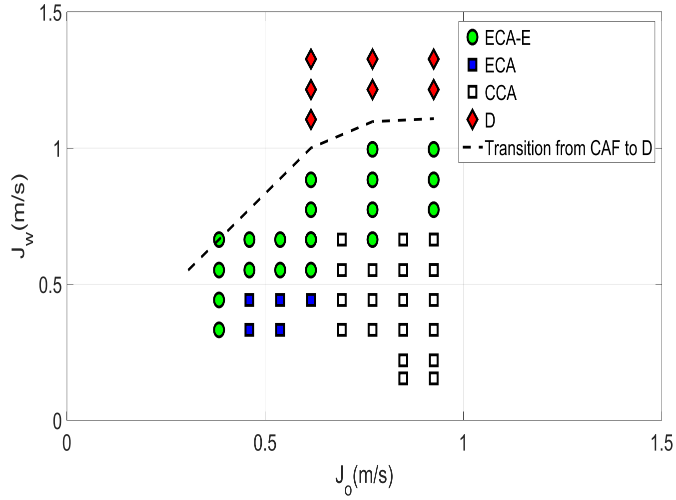

(b)

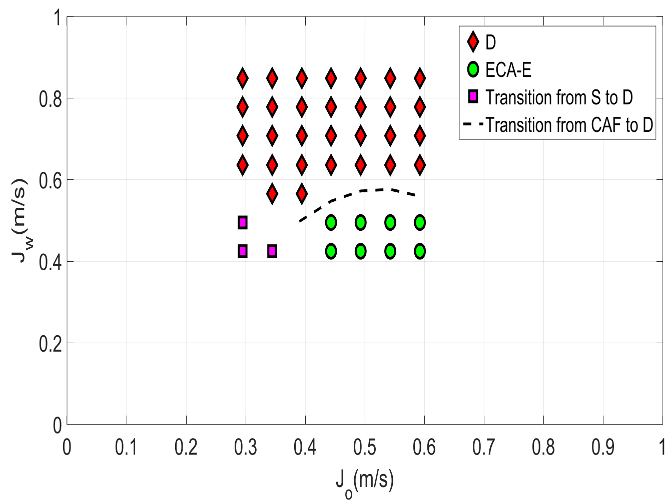

(c)

Fig. 2. Flow regime maps for three cases of downstream sudden expansion. a) 21-30 mm (TS2), b) 30-40 mm (TS3), c) 30-50 mm (TS4)

4.1.2 Comparison of flow pattern map with literature data bank

Among many works performed on liquid-liquid flow, Sotgia et al. (2008) reported flow pattern maps for very viscous oil-water flow in horizontal straight pipes, using the same oil and a 26 mm i.d. pipe. Transition boundaries between the different flow patterns were investigated in this paper, showing that there is a region between CAF and fully dispersed flow with transitional characteristics. Owing to the very similar upstream diameter (26 mm compared to 30 mm), the data regarding the downstream pipe of TS2 can be reasonably compared in order to understand the flow pattern variation caused by the sudden expansion. Fig. 3 (a) and 3 (b) show a comparison of flow pattern maps developed in the current study regarding 30 mm i.d. pipe downstream of 21-30 mm and that available from Sotgia et al. (2008) in the 26 mm i.d. straight pipe, represented respectively with (J_o, J_w), and (ε_w, J_m) coordinates. For the sake of comparison, these two representations turn out to be equivalent. Two flow regimes are observed downstream of the sudden expansion 21-30 mm pipe, i.e. CAF and dispersed flow. Furthermore, the transition boundary lines from CAF to D flow is illustrated by the dashed line in the presence of sudden expansion. The figures include the flow regimes observed in the work of Sotgia et al. (2008) together with the transition boundaries (solid lines). It is evident that CAF flow in the current study is overlapped to the CAF region reported by Sotgia et al (2008). In both cases, a transition from CAF to D flow regime occurs principally by increasing the water superficial velocity. The major difference between the two flow pattern maps is that owing to the sudden expansion the region of CAF is reduced whereas the region of dispersed flow is increased. Actually, dispersed flow downstream of the area change (shown in red marker) is observed to occur far below the transition line from CAF to D observed by Sotgia et al (2008). For the straight pipe it is more difficult to compare trends of CAF to D transition boundary because the lack of data with J_o>0.97 $m{\cdot}s^{-1}$ in Sotgia et al. (2008). In any case, in the range $0.6<J_o<1$ $m{\cdot}s^{-1}$ it is observed a similar behavior with increasing with J_o.

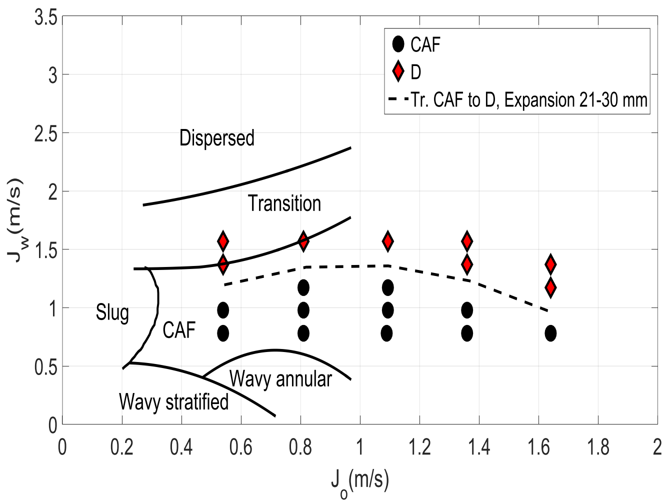

(a)

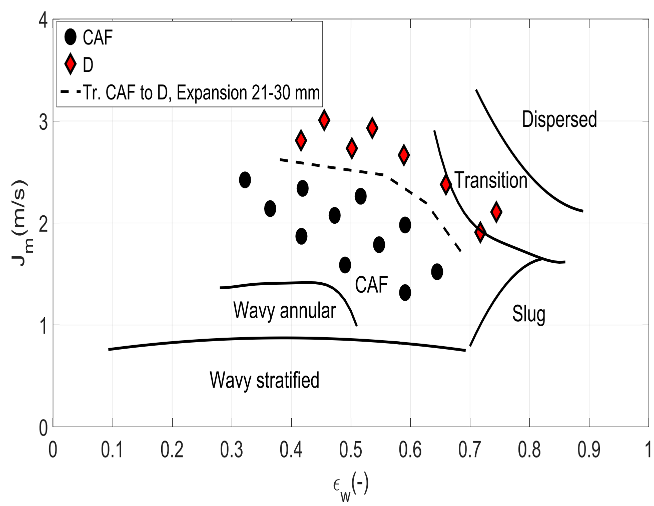

(b)

Fig 3. Comparison of flow pattern map of downstream the sudden expansion 21-30 mm and Sotgia et al (2008) with D=26 mm. Flow regimes regarding 30 mm downstream of sudden expansion are shown in markers. Solid lines are transition lines between different flow regimes in Sotgia et (2008). Dashed lines represent transition from CAF to D in 30 mm i.d. pipe downstream of sudden expansion 21-30 mm. (a) J_o and J_w as coordinates; (b) ε_w and J_m as coordinates.

4.2 Distributed pressure gradient

As water lubricated flow is an effective method to transport heavy oil, it is also important to assess the influence of geometrical singularities which are likely to be present in a pipeline. A key point is to understand if the disturbance introduced by the pipe element can significantly alter the pressure drop. In this section, the results of two-phase pressure gradients for different pipe configurations are presented because pressure gradients are required to compute concentrated (singular) pressure drop as well as two-phase loss coefficient, as it will be shown in Section 4.3. It is interesting to try to relate the pressure gradient along the ducts downstream of singularities to the flow patterns, as seen as an example in Fig. 4, where three cases of sudden expansion, e.g. 21-30 mm, 30-40 mm, and 30-50 mm are considered. Apart from pipe configuration, core-annular flow regime provides the lowest pressure gradient as compared to dispersed flow regime. Moreover, by comparison of sudden expansion 21-30 mm and 30-50 mm, one may find out that pressure gradient is significantly reduced.

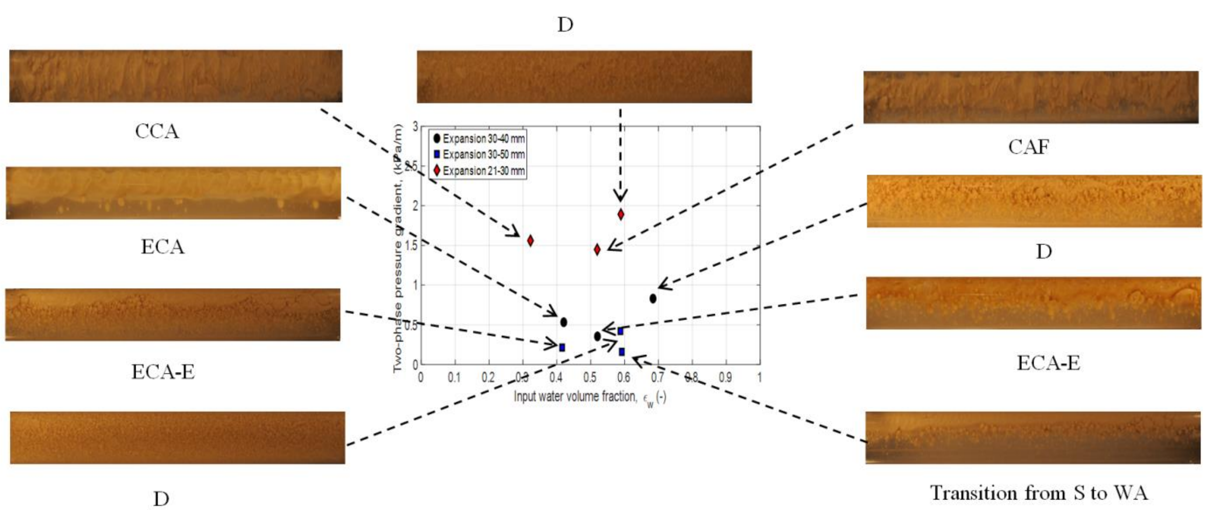

Fig 4. Typical pressure gradient versus input water volume fraction and corresponding flow pattern for all cases of sudden expansion

The parametric investigation is conducted making use of the pressure gradient as a function of water input volume fraction. One case of sudden contraction (TS1: 30-21 mm) and three cases of sudden expansion (TS2: 21-30 mm, TS3: 30-40 mm, and TS4: 30-50 mm) are considered in the analysis of pressure measurements. The typical trends of distributed pressure gradient with input water volume fraction (ε_w), parameterized by superficial oil velocity (J_o) are depicted in Fig 5 and Fig 6. Fig 5 shows the results of pressure gradient measurement in case of sudden contraction both upstream and downstream, while Fig 6 shows the measured pressure gradient for the three cases of sudden expansion. For the pipe downstream of the sudden expansion, the corresponding flow patterns are also shown in Figs 6 (a-c). Shi (2015) proved that for very viscous oil-water flow, the transition from water-continuous to oil-continuous (phase inversion) occurs for input water volume fraction lower than 40%, depending on oil superficial velocity. It is also indicated that the stable water-lubricated flow can be developed at a lower ε_w with increase of oil superficial velocity. Accordingly, the investigated operating conditions correspond to a stable water-lubricated flow and are favorable for transport of heavy oil. Fig. 5 shows the same trend of pressure gradient as a function of input water fraction both upstream and downstream of sudden contraction, that is, pressure gradient increases as input water fraction increases for fixed amount of oil. This is not surprising because increasing water superficial velocity would contribute to increase wall shear stress and finally pressure gradient. The magnitude of pressure gradient is higher downstream than upstream because of the higher magnitude of superficial velocity in the downstream pipe.

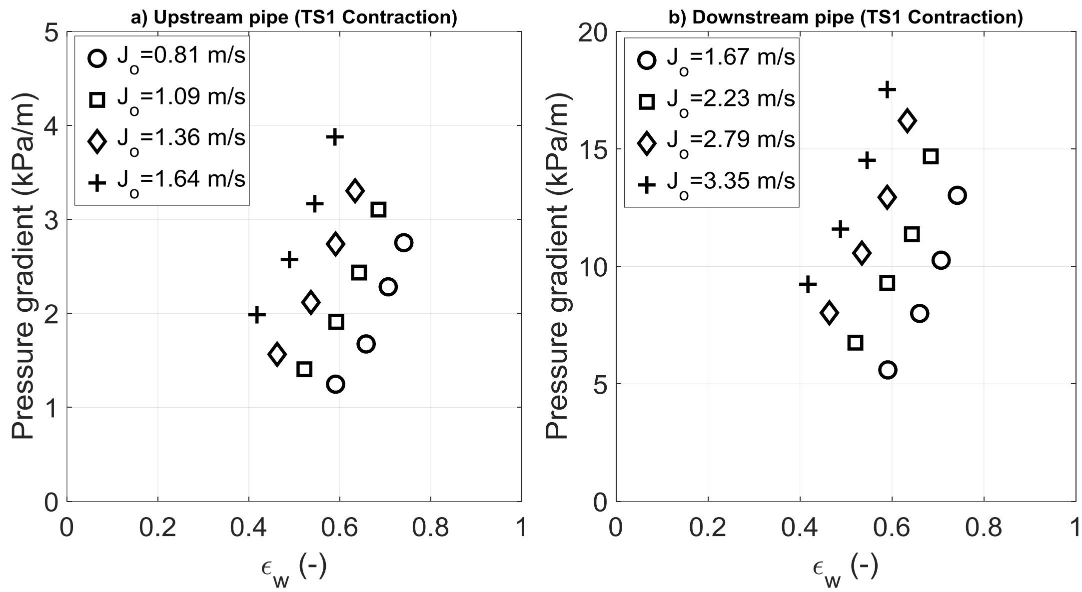

Fig. 5 The trend of pressure gradient measurement as a function of input water volume fraction; a) upstream pipe (TS1, contraction), b) downstream pipe (TS1, contraction)

Similar trend but different magnitude of the pressure gradient as a function of the water input volume fraction is observed for the all cases of sudden expansion. In Fig 6 (a-c), different symbols indicate the observed flow regimes, while different colors represent the oil superficial velocities. From inspection, it is evident that core-annular flow is obtained at the lower values of input water volume fraction, while increasing water flow rate would result in transition from core-annular to dispersed flow. It can be noted also that no considerable deviation is observed for different sudden expansion configurations. Almost the same qualitative trend of the pressure gradient as a function input water volume fraction is observed downstream of the geometrical singularity. Moreover, core-annular flow always shows the lowest pressure gradient downstream of the sudden expansion.

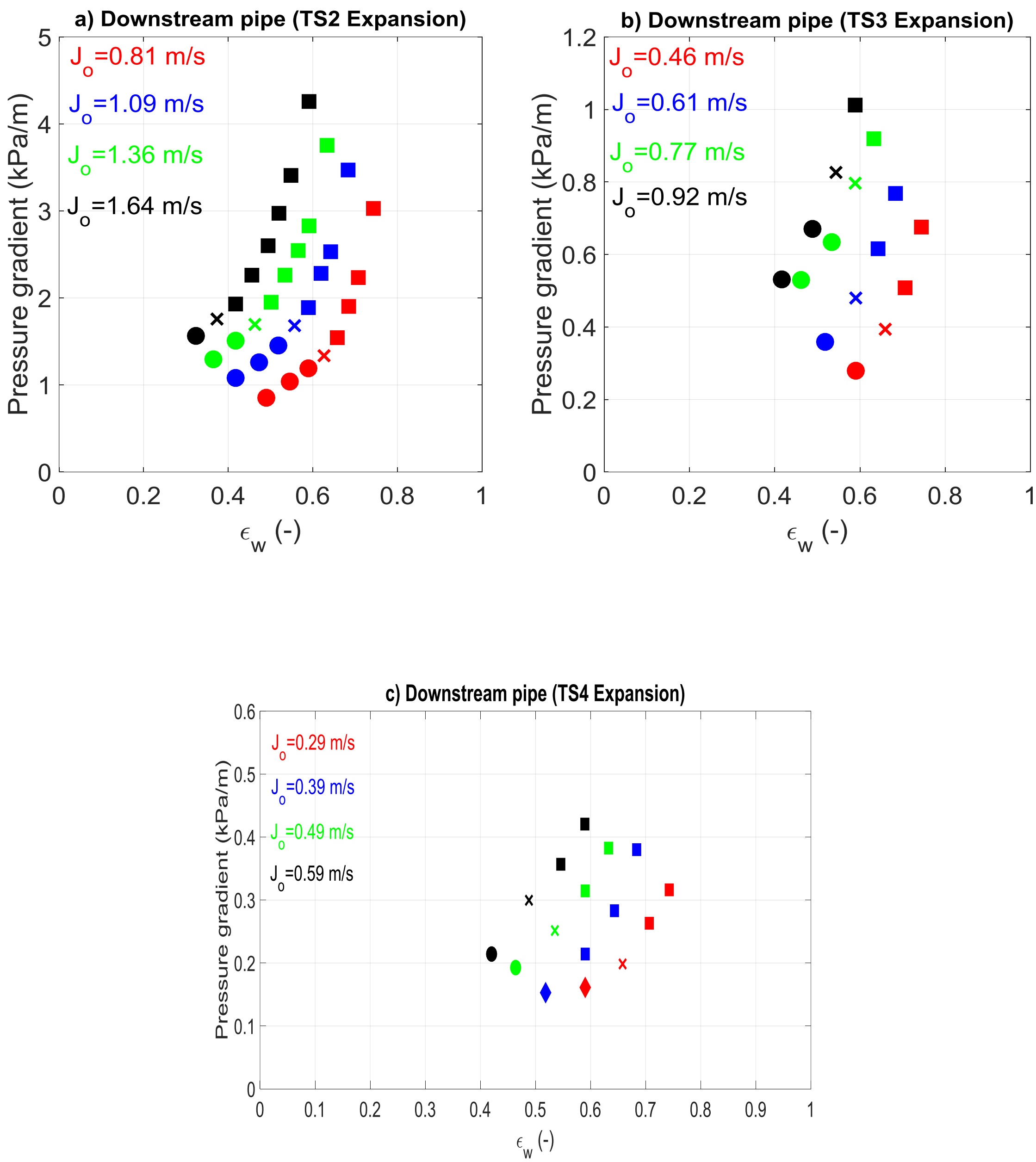

Fig 6 Trend of the measured pressure gradient as a function of input water volume fraction; a) downstream pipe (TS2, expansion), b) downstream pipe (TS3, expansion), c) downstream pipe (TS4, expansion). o:CAF, x:transition from CAF to D, ⊓: D, ◊: transition from S (stratified) to CAF.

Pressure behaviors along the pipe are represented in Fig 7 (a-d). Fig 7-a shows the results for contraction TS1, whereas Fig 7 (b-d) presents the three case of sudden expansion, e.g. TS2, TS3 and TS4, respectively. In all figures the measured two-phase pressure drop (ΔP_{ow}) is plotted as a function of tap distance (L) from the plane of singularity, normalized by pipe diameter (L/D). The lowest and highest mixture superficial velocities (J_m) are considered for the sake of comparison. Regarding the flow through contraction TS1, the pressure gradient increases both upstream and downstream of the plane of area change, with steeper slope downstream of singularity, which is due to the higher mixture superficial velocity. In fact, from the point of contraction, both frictional loss and sudden area change contribute to the steeper pressure gradient downstream of TS1. In the upstream pipe of TS1, pressure profiles are less dependent on mixture superficial velocity and water input volume fraction. Similar trend is observed for three cases of expansion TS2, TS3, and TS4. The pressure profiles upstream of expansion have steeper slopes than the downstream pipe due to the larger mixture velocity in the former case. Moreover, in all expansion cases, the two-phase pressure drop increases along the length of the pipes. The behavior of pressure profiles downstream of expansion is of complex interpretation. Actually, pressure gradients for TS2 and TS3 are highly dependent on mixture superficial velocity and input water volume fraction, while this is not observed for TS4. The trends of pressure profiles shown in Fig 7 (a-d) are in agreement with the reported results of Hwang and Pal (1997) and Balakhrisna et al. (2010) who used oils with much lower viscosity. Unfortunately, there is no information regarding pressure profiles for a very viscous oil-water flow through singularity in the previous studies to compare our results.

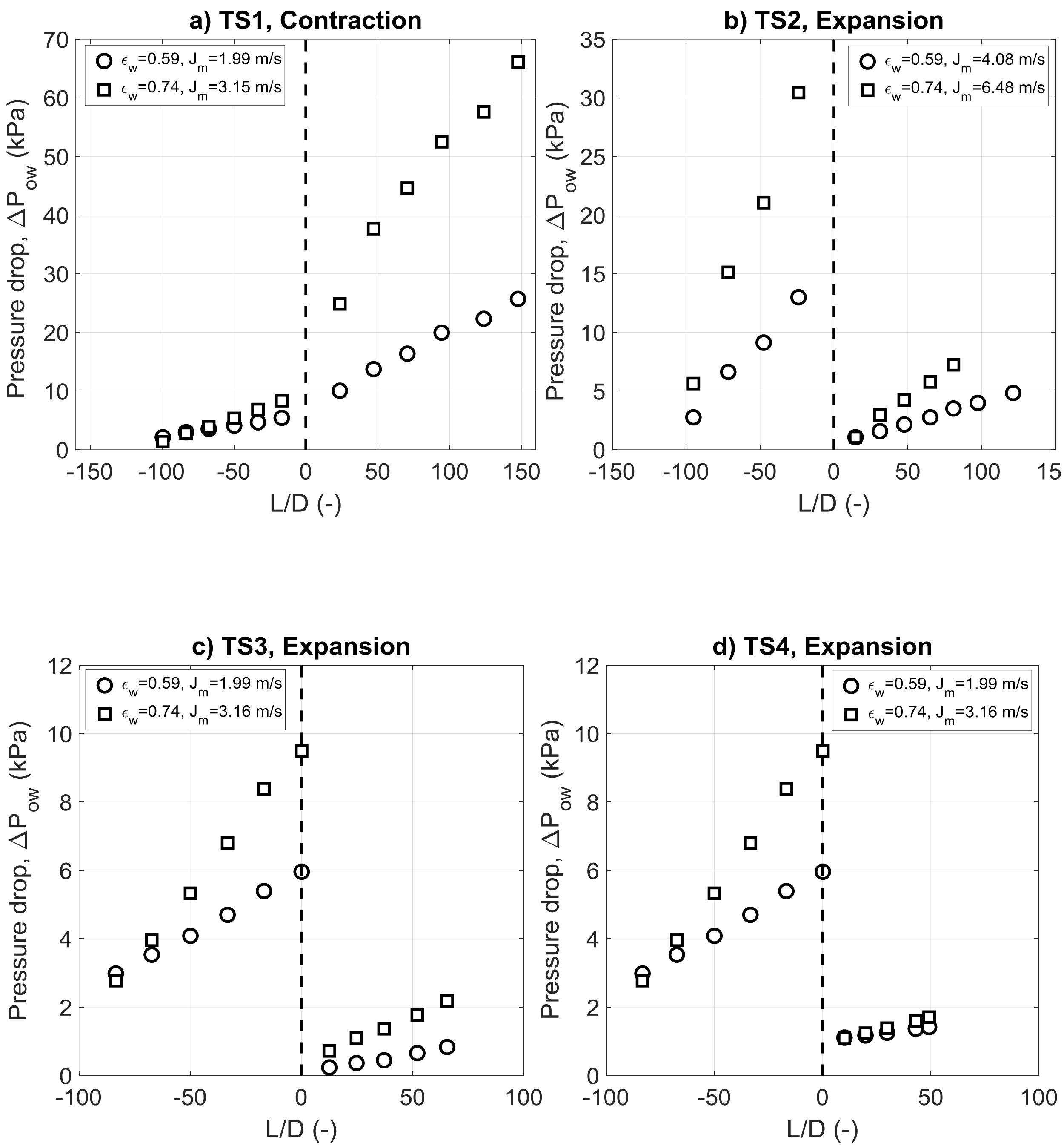

Fig 7 Pressure profiles along the pipe, a) sudden contraction TS1, b) sudden expansion TS2, c) sudden expansion TS3, d) sudden expansion TS4.

4.3 Method of pressure gradient

The influence on flow characteristics of the change in pipe cross-section can be quantitatively addressed by evaluating the concentrated pressure drop across the singularity. This can be calculated by the pressure gradient technique which does not involve direct measurement. Actually, it is based on extrapolation of the pressure profile relative to the fully developed flow upstream and downstream of the pipe up to the plane of the geometrical singularity. In such a plane a it is then found a discontinuity in the pressure, which is the concentrated pressure drop (ΔP_s). Fig 8-a (TS1) and 8-b (TS2) show ΔP_s as a function of the input water volume fraction (ε_w) , at constant oil superficial velocity. As expected, the concentrated pressure drop increases as the water content increases at the same oil superficial velocity and it also increases at constant water input volume fraction at growing oil superficial velocity. Both the contraction and the expansion show a similar behavior.

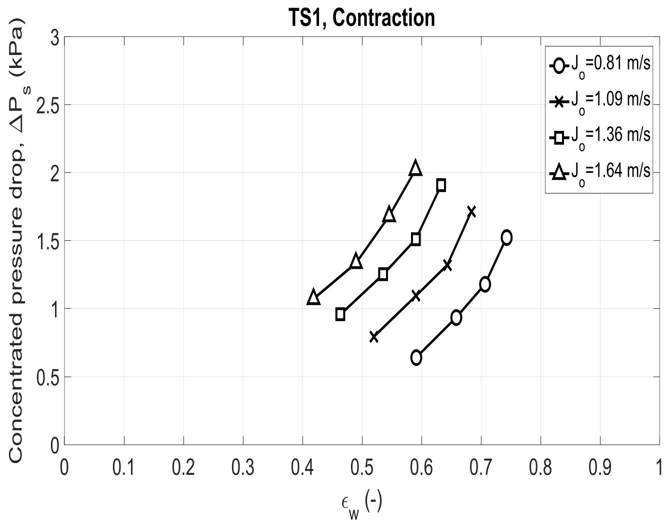

(a)

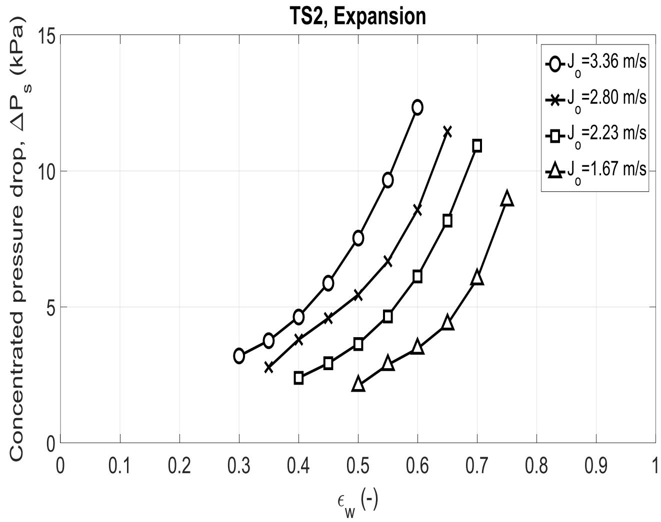

(b)

Fig 8. Concentrated pressure drop (ΔP_s) versus input water volume (ε_w) in different oil superficial velocity for a) TS1, b) TS2

From the mechanical energy equation, the concentrated pressure drop is used to evaluate the energy loss coefficient. In particular, for an abrupt expansion, denoting by subscripts 1 and 2 upstream and downstream pipes, respectively, it follows:

$$h_f = -\frac{\Delta P_S}{\rho_m \frac{J_{m-1}^2}{2}} \frac{J_{m-1}^2}{2} + \left[1 - \left(\frac{D_1}{D_2}\right)^4\right] \frac{J_{m-1}^2}{2} = (-k_1 + k_2) \frac{J_{m-1}^2}{2} = k_{tot} \frac{J_{m-1}^2}{2}, \qquad (14)$$

Where,

$$k_1 = \frac{\Delta P_S}{\rho_m \frac{J_{m-1}^2}{2}} \qquad (15)$$

is the loss coefficient due to irreversibility, i.e. mechanical energy degradation;

$$k_2 = \left[1 - \left(\frac{D_1}{D_2}\right)^4\right] \qquad (16)$$

takes into account the geometrical configuration of the sudden change of cross-sectional area;

$k_{tot} = k_2 - k_1$ (17)

is the total loss coefficient. The stronger the change in the cross-section area, the larger is k_2 as well as its impact on the total loss coefficient compared to k_1. It is worth noting that, since the difference in the fluid densities is relatively small, the mixture density ρ_m appearing in Eq. (14) is reasonably approximated as the homogeneous density, as assumed in all the works presented in the literature:

$$\rho_m = \varepsilon_w \rho_w + \varepsilon_o \rho_o \quad (18)$$

Accordingly, it has to be stressed that the definition of k_{tot} is merely conventional and related to the assumption of homogeneous flow, which is not generally verified. Hence, k_{tot} is simply an empirical parameter, useful to calculate ΔP_s in a simple way.

.. For a sudden contraction, Eq. 14 still holds provided that the signs of both terms on the right side are reversed.

Since the value of k_2 is constant for a fixed geometrical configuration, only the results for k_1 will be presented and discussed. Fig 9 (a-c) represents k_1 versus the mixture superficial velocity in the upstream pipe, $J_{m\text{-}up}$. In all figures, different marker colors correspond to different superficial oil velocities. It is worthwhile mentioning that all data crowd up quite well into a unique trend, irrespective of the superficial oil velocity. However, the behaviors are different and it is difficult to provide an explanation of their peculiarities. In particular, for TS1 and TS2, an almost constant behavior is observed, with a value of the loss coefficient for the abrupt contraction TS1 lower than for the abrupt expansion TS2. On the contrary, the abrupt expansion TS4, with the highest cross-section area ratio, clearly shows a decreasing trend of k_1 with the mixture velocity. This seems consistent with the behavior of the pressure gradient observed in Fig. 7 (d), showing slight changes in the downstream pipe, but the physical meaning is still unclear. We cannot exclude that the assumption of homogeneous flow implicit in Eq. (14) is responsible for non-physical trends, in which case, as already mentioned above, k_1 and hence k_{tot} are merely empirical parameters only useful to calculate the concentrated pressure drop.

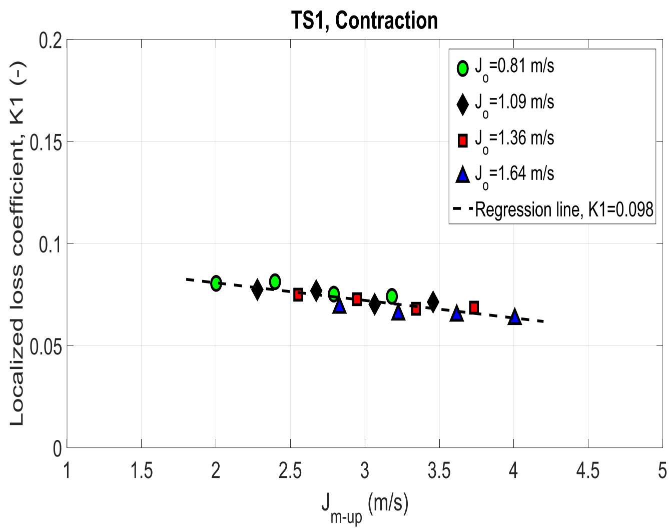

(a)

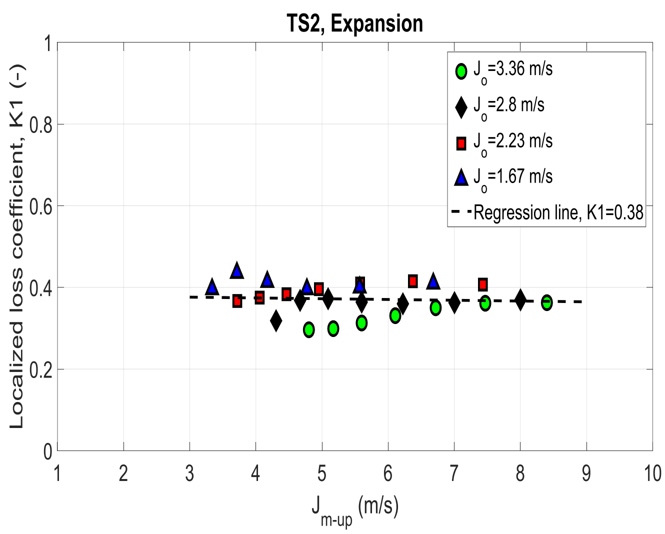

(b)

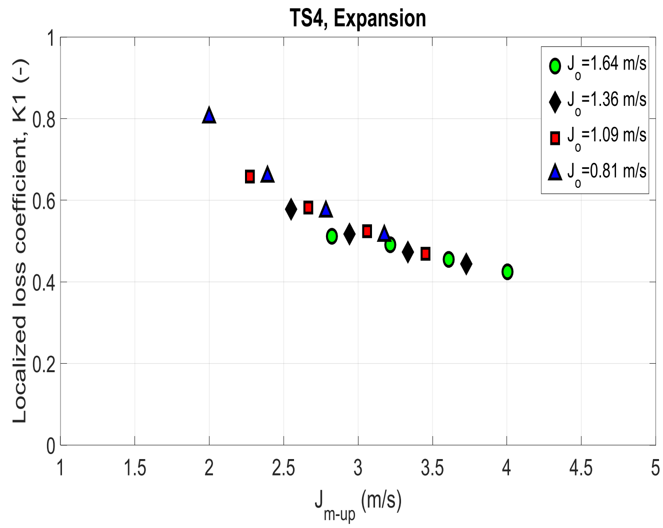

(c)

Fig. 9 The localized loss coefficient (k_1) as a function of mixture volumetric flux upstream of singularity for a) TS1, b) TS2, and c) TS4

Moreover, an attempt was made to compare the total loss coefficient values (k_{tot}) with the reported values in the literature survey. Several researchers proposed empirical correlations to compute the loss coefficients for single-phase flow through abrupt contraction and expansion. On the other hand, there are only two experimental works, which reported the total loss coefficients in liquid-liquid flows. Hwang and Pal (1997) used very low viscosity oil and the main flow regimes was reported as oil-in-water and water-in-oil emulsion. Balakhrisna et al. (2010) used two types of oils, which included lube oil (μ_o=0.2 Pa·s and ρ_o=960 kg/m^3) and kerosene (μ_o=0.0012 Pa·s and ρ_o=787 kg/m^3). Tables 6-a and 6-b listed the results of the total loss coefficients through contractions and expansions in the present experiment as well as the comparison with previous experimental data and empirical correlations. It is evident that in the literature models the effect of fluid properties has not been taken into account because the total loss coefficient is only presented as a function of diameter ratios. Table 6-a shows a wide range of the loss coefficient for sudden contractions varying from 0.20 by McCabe et al. (1993) to 0.68 by Chisholm (1983). On the other hand, k_{tot} in the present experimental data is quite similar to the one measured by Balakhrisna et al (2010). In Table 6-b dealing with the sudden expansion it is seen a better agreement with most of the experimental data, apart from the work by Hwang and Pal (1997). However, the latter deals with emulsions obtained from water and low-viscosity oil, i.e. a system strongly different from the one considered in the present work. Eventually, available models largely fail in predicting the loss coefficient.

Table 6-a Total loss coefficient for sudden contraction TS1

From experiment	Reported in the literature by				
	Chisholm (1983) $k_{tot} = \frac{1}{[0.639\,(1-\varsigma^2)^{0.5}+1]}$	McCabe et al. (1993) $k_{tot} = 0.4\,(1-\varsigma^2)$	Hwang and Pal (1997)	Balakhrisna et al. (2010) Kerosene-water	Balakhrisna et al. (2010) Lube oil-water
0.45	0.68	0.20	0.54	0.38	0.48

Table 6-b Total loss coefficient for sudden expansion TS2

From experiment	Reported in the literature by				
	Borda-Carnot $k_{tot} = (1-\varsigma^2)^2$	Wadle (1989) $k_{tot} = 2\varsigma^2\,(1-\varsigma^2)$	Hwang and Pal (1997)	Balakhrisna et al. (2010) Kerosene-water	Balakhrisna et al. (2010) Lube oil-water
0.37	0.26	0.49	0.47	0.4	0.43

4.4 Holdup prediction

From Table 5 it can be concluded that eccentricity of oil core plays an important role downstream of the sudden expansion with the highest cross-section area ratio. This effect should be stronger lowering the oil superficial velocity, because the water layer between top of oil core and internal pipe diameter becomes thinner and thinner according to visual observations, increasing the drag force exerted on the oil core. Shi et al. (2017) proved that for viscous oil-water mixture when oil superficial velocity increases, within a wide range of superficial water velocities, the oil core is more and more concentric . Hence, phase holdup is not only affected by the flow rates (or input volume phase fractions) but also by oil core eccentricity. Its degree can be taken into account by the dimensionless Froude number, $\mathrm{Fr} = \frac{J_o}{\sqrt{gD\frac{\rho_w-\rho_o}{\rho_o}}}$, which represents the ratio between inertia to buoyancy forces. Evidently, when the oil core is more eccentric the action of buoyancy is increasingly important compared to inertial effects. Arney et al. (1993) correlation, $H_w=\varepsilon_w[1+C(1-\varepsilon_w)]$ with C=0.35, for prediction of phase holdup has been developed for almost concentric oil core (D=16 mm), and its validity has not been confirmed for larger pipe diameter downstream of sudden expansions, where, as noticed above, eccentricity is very evident. Colombo et al. (2017) validated Arney et al. (1993) correlation with larger amount of data-set for pipe diameters of D=21 mm, D=30 mm, and D=40 mm, and obtained C=0.36, which is practically the same as the coefficient determined by Arney et al. (1993). They found a very good agreement between the model and experimental data of QCV downstream of sudden contraction. However, they observed that the predictions worsen as the pipe diameter increases and concluded that oil core eccentricity should be taken into consideration. Therefore, a modified correlation of Arney et al. (1993) is proposed in the following, based on the experimental data of Colombo et al. (2015) for D=30 mm and D=40 mm downstream of sudden contraction. The schematic of oil core eccentricity is depicted in Fig. 10.

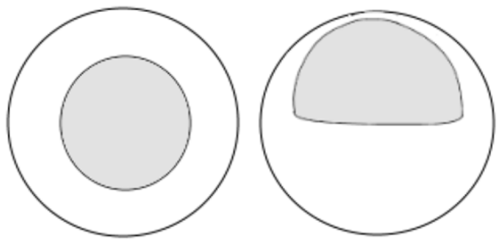

Fig 10. Schematic of oil core eccentricity

In analogy with the investigation performed by Shi et al. (2017), the functional form for oil holdup is expressed as:

$$H_o = 1 - \varepsilon_w[1 + 0.36(1 - \varepsilon_w)]E \qquad (19)$$

$$E = e^{-a\left(\frac{1}{Fr}\right)^{b}(\varepsilon_o)^{c}} \qquad (20)$$

$$\frac{1}{Fr} = \frac{\sqrt{gD\frac{\rho_w - \rho_o}{\rho_w}}}{J_o} \qquad (21)$$

From non-linear regression on two data-sets from Colombo et al. (2015, the values of a = 0.1, b = 0.94, and c = 1.07 are obtained. The coefficient E, is introduced to consider the effect of oil core eccentricity, which is a function of input oil volume fraction (ε_o) and the inverse of Froude number. Eq. (19) was proposed because the validity of Arney et al. (1993) correlation has been already confirmed against a very wide database (see e.g. Arney et al., 1993, Colombo et al., 2015, and Shi et al., 2017). The physical meaning is explained as follows. The eccentricity coefficient (E) takes values between 0 and 1: in particular, the lower the Froude number, the more pronounced the eccentricity; accordingly, E tends to unity; conversely, the higher the

Froude number, the more concentric the oil core, thus E tends to zero. Moreover, as mentioned by Shi et al. (2017), the inverse of Froude number is introduced to involve the case of 1/Fr = 0 when the fluids are density matched ($\rho_o = \rho_w$, E = 1).

Fig. 11-a and 11-b show the oil holdup as a function of the oil input volume fraction for the pipes with D=30 mm and D=40 mm, respectively, downstream of a sudden contraction as reported by Colombo et al. (2015). Furthermore, prediction of the oil holdup from available models in the open literature is also shown. The dashed lines represent homogeneous flow (the average actual velocities of oil and water are equal). It is evident that the measured oil holdup data are located below the bisector (oil holdup is lower than input oil volume fraction), meaning that oil moves faster than water. From Fig. 11 it can be observed that the model by Oliemans et al. (1987) always overestimates the data with mean average percentage errors (MAPE) of 23.5 % and 19.5 % for D=30 mm and D=40 mm, respectively. The mechanistic models by Brauner (1998) and Ullmann and Brauner (2004) predicted oil holdup with better accuracy. The statistical performance of the models is reported in Table 7. The empirical correlation by Colombo et al. (2015) was not mentioned in Table 7 due to the fact it practically produces the same result as Arney et al. (1993) with the minor difference in the coefficient, C. The Shi et al. (2017) model with updated coefficients (proposed model) is able to predict the oil holdup in a very good agreement with experimental data regardless of concentric or eccentric oil core (92 % of all data fall within ±5 % of relative error). A comparison of the model prediction and experimental data of Charles et al. (1961) is depicted in Fig. 12, showing a satisfactory agreement with MAPE=12.2 %. It is worth remarking that Charles et al. (1961) used a density matched oil and water mixture, flowing through a small pipe diameter (D=26 mm and μ_o=0.016 Pa·s), therefore, the oil core is almost concentric and eq. 6 reduces to Arney et al. (1993) correlation with E=1.

Another attempt was made to evaluate the performance of the proposed model with measured data of Shi et al. (2017) who used oil-water mixture with much more viscous oil (μ_o = 5 Pa·s), flowing within 25.4 mm i.d. duct (see Fig. 13). They observed eccentric core flow with oil fouling in some operating conditions, which explains the data with $H_o > \varepsilon_o$ (the oil in contact with the wall moves slower than the water). Furthermore, the rest of the data, showing $H_o = \varepsilon_o$, very likely refer to the onset of the transition between eccentric-core annular flow and stratified-wavy flow. Accordingly, these data represent the limit of application of the proposed model (corresponding to the lower limit of the Froude number, below which core flow does not exist anymore). A fairly good agreement is shown between oil holdup predicted by the proposed model and experimental data of Shi et al. (2017) with MAPE=16.5 %.

From the above discussion, it can be concluded that the correlation of Arney et al. (1993) modified according to Shi et al. (2017) in order to consider the influence of core eccentricity significantly improves the prediction of oil holdup.

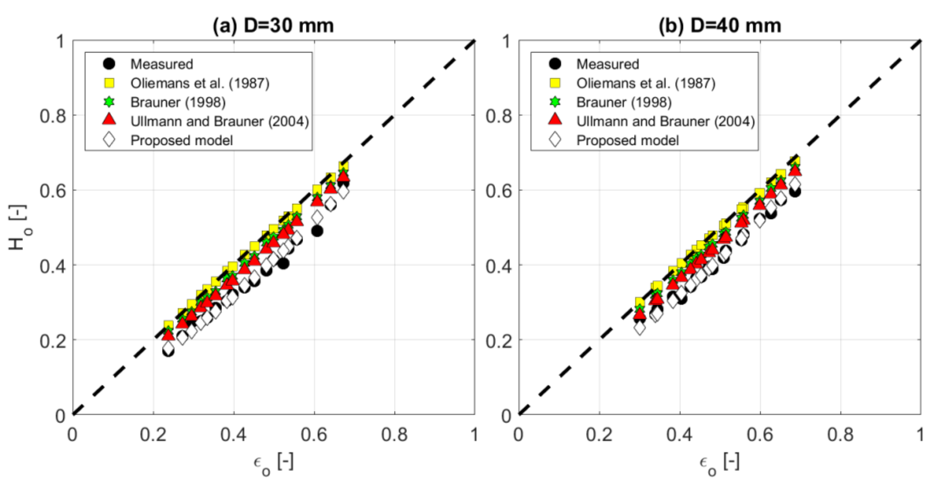

Fig. 11 Oil holdup versus input oil volume fraction for downstream of sudden contraction with (a) D=30 mm and (b) D=40 mm (Comparison between experimental data of Colombo et al. (2015) and available models in the open literature)

Table 7 Statistical performance of the available models in the literature to predict oil holdup

Author	Average relative error (%)	Max relative error (%)	Min relative error (%)	MAPE (%)	St. deviation (%)
Oliemans et al. (1987)	21.5	39.4	7.3	21.5	6.1
Arney et al. (1993)	-0.8	8.0	-11.9	2.7	3.7
Brauner (1998)	15.3	30.5	4.2	15.3	4.9
Ullmann and Brauner (2004)	11.4	22.9	2.5	11.4	4.1
Proposed model	0.1	7.9	-9.9	2.5	3.6

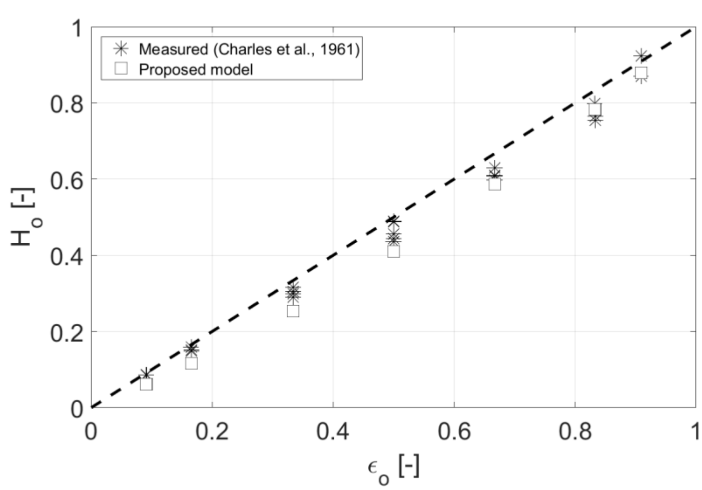

Fig. 12 Oil holdup versus input oil volume fraction, comparison of the proposed model and experimental data of Charles et al. (1961) with μ_o=0.016 Pa·s

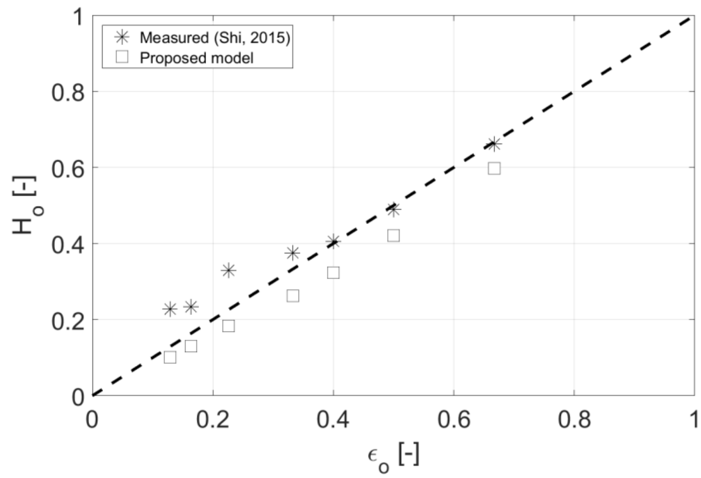

Fig. 13 Oil holdup versus input oil volume fraction, comparison of the proposed model and experimental data of Shi et al. (2017) with μ_o=5.0 Pa·s

4.5 Pressure drop estimation

Once a suitable expression for the water holdup (H_w=1-H_o) is found from Eqs. (19)-(21), the proposed formulation of the two-fluid model by Colombo et al. (2017), i.e., Eq. (13) can be used to predict the pressure drop. Experimental data on the pressure drop for viscous oil-water mixture both upstream and downstream of the cross-section area change are used in the present study to validate the prediction by the literature models described in Section 2. The available database contains 120 data points. Prediction of pressure gradients by Arney et al. (1993), Brauner (1998), together with the proposed model are reported in Figs. 14 (a-d) to 16 (a-d), respectively. In each Figure, the predicted pressure gradient is compared with the measured one for ducts with internal pipe diameters: (a) D=21 mm, b) D=30 mm, c) D=40 mm, and d) D=50 mm. The models by Arney et al. (1993) and Brauner (1998) give a quite similar prediction of the pressure gradients. Both models overestimate the measured pressure gradient for pipe diameters

21 mm, 30 mm, and 40 mm. However, they underestimate the measured pressure gradient for D=50 mm. The performance is in any case satisfactory, with 80% and 87% of data falling within ±30 % relative error for Brauner (1998) and Arney et al. (1993), respectively. Specifically, the model by Arney et al. (1993) shows slightly better performance than Brauner (1998) model in the whole range of flow conditions under investigation.

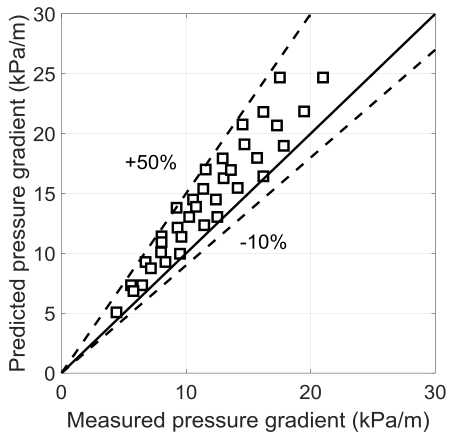

(a)

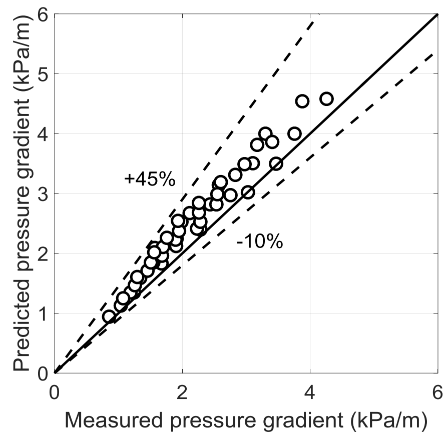

(b)

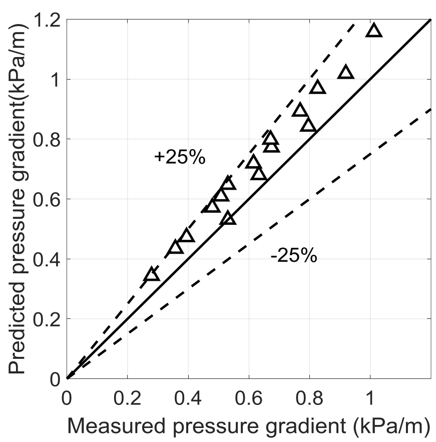

(c)

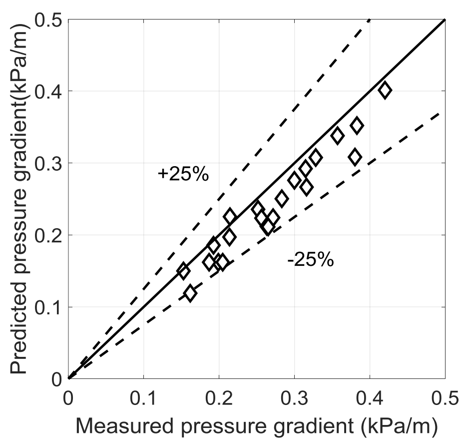

(d)

Fig. 14 Comparison between measured pressure gradients and prediction from Arney et al. (1993) for a) D=21 mm, b) D=30 mm, c) D=40 mm, and d) D=50 mm

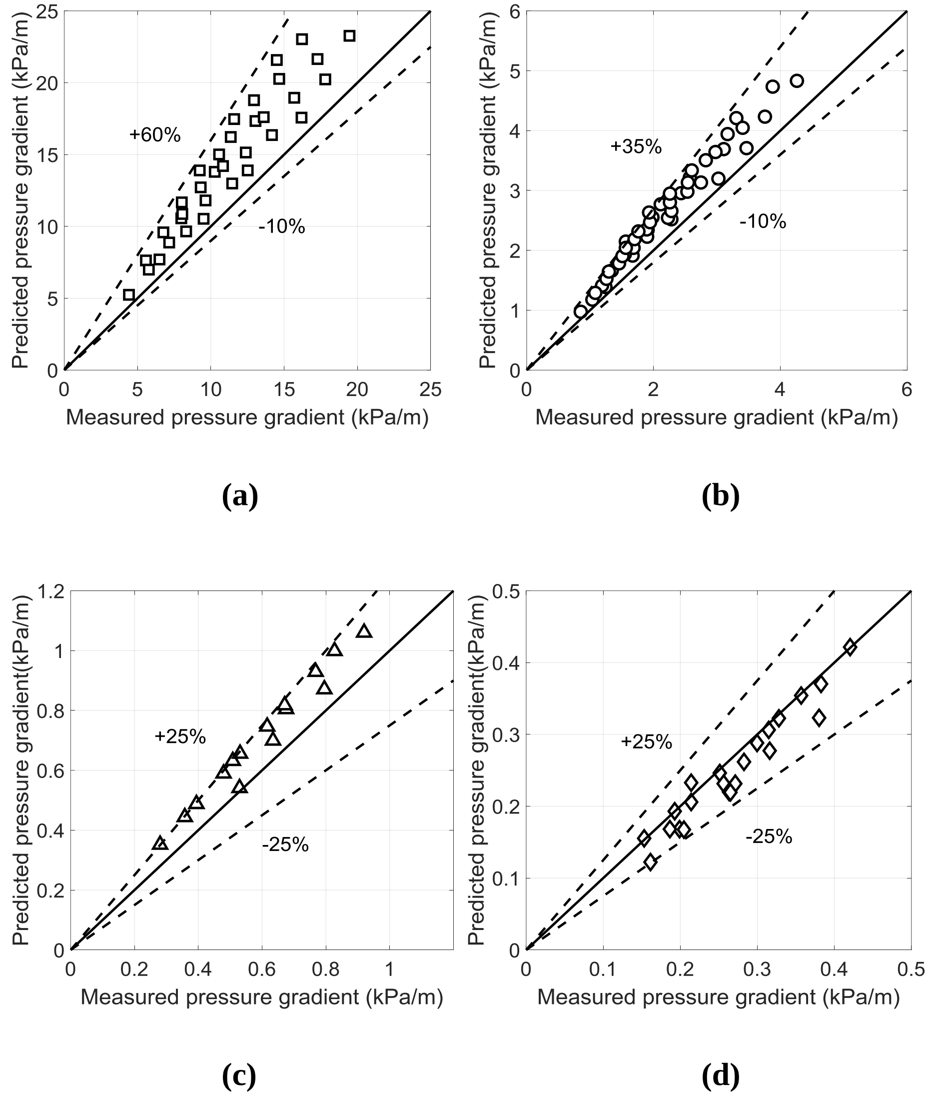

Fig. 15 Comparison between measured pressure gradients and prediction from Brauner (1998) for a) D=21 mm, b) D=30 mm, c) D=40 mm, and d) D=50 mm

A comparison between the measured pressure gradient and the prediction from the model proposed in the current study is depicted in Fig. 16 (a-d). Overall, 93 % and 98 % of the data fall within ±20 % and ±25 % of relative error, respectively. The improvement in the prediction is related to the fact that an empirical expression of the water holdup has been adopted instead of a theoretical expression for the interfacial shear stress as a closure relationship for the Two-Fluid model, as suggested by Colombo et al. (2017). Here, the further improvement consists of accounting for the oil-core eccentricity, as explained in Section 4.4. Table 8 shows in summary the statistical analysis of the performance for the selected models.

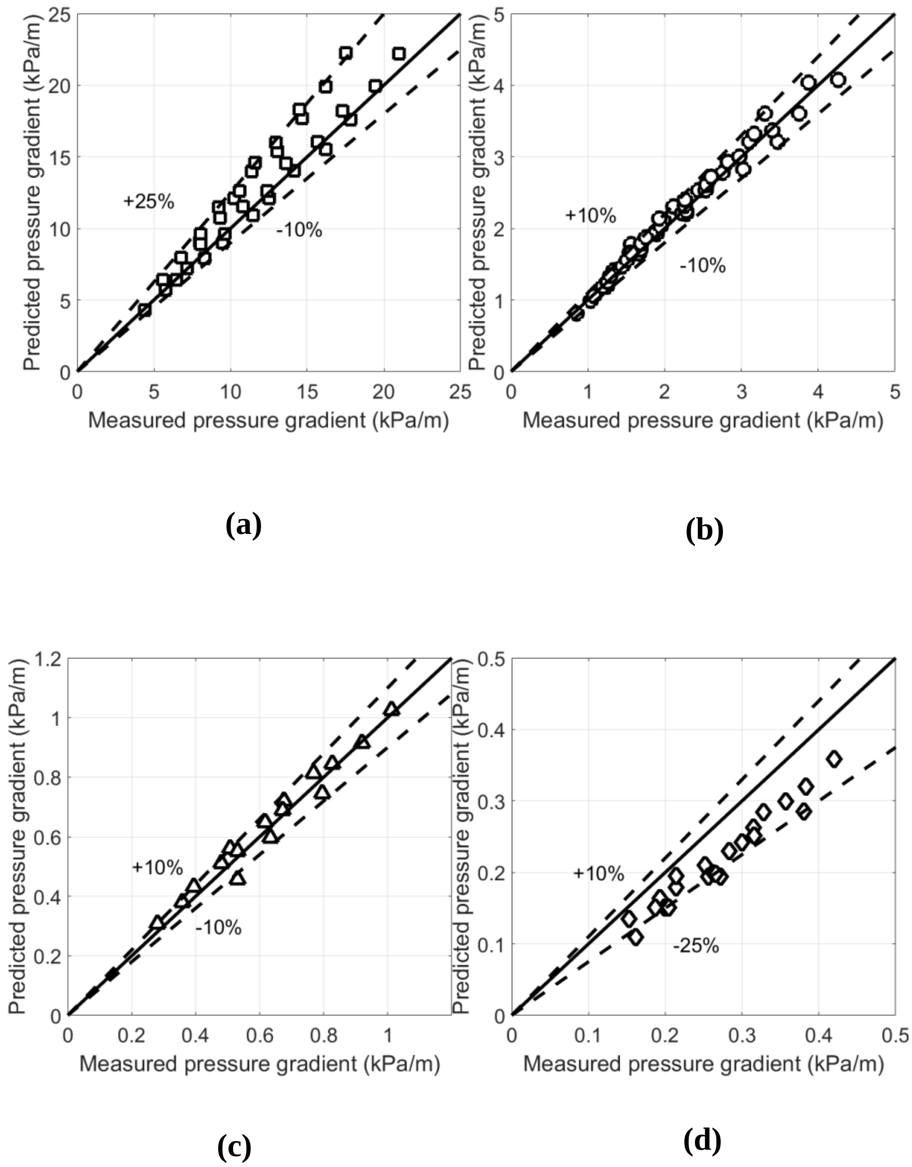

Fig. 16 Comparison between measured pressure gradient and prediction from the proposed model in the current study for a) D=21 mm, b) D=30 mm, c) D=40 mm, and d) D=50 mm

Table 8 Statistical analysis of the performance of available pressure gradient models for viscous oil-water flow

Model	Average relative error (%)	Maximum relative error (%)	MAPE (%)
Arney et al. (1993)	13.7	49.5	17.9
Brauner (1998)	18.3	50.0	21.3
Proposed	0.4	23.5	9.3

5 Conclusion

Experimental results on viscous oil-water horizontal flow in the presence of sudden contractions and expansions were reported regarding flow patterns, distributed pressure gradient, concentrated pressure drop, and phase holdup. The most significant achievements are briefly highlighted in the following:

- The main flow patterns observed downstream of sudden expansions for viscous oil-water flow included dispersed oil-in-water (D), Core-annular flow (CAF), Corrugated Core-annular flow (CCA), Eccentric Core-annular with and without drop entrainment (ECA-E and ECA), transition from CAF to D flow, transition from Stratified (S) to D, and transition from S to CAF flow. According to the visual inspection, the stronger the cross-section area change (in the present work, TS4), the more intense the influence on oil core eccentricity downstream of the sudden expansion with increased disturbances at the oil-water interface. The proper choice of the area ratio is crucial in the presence of sudden expansions because excessive area ratios might determine contact of oil with the wall (oil fouling) in the downstream pipe and, hence increased pressure gradient.

- Flow pattern maps were developed for the pipes downstream of sudden expansions TS2 (21-30 mm), and TS3 (30-40 mm), and TS4 (30-50 mm) to evaluate the effects of different area ratios on flow pattern. It was concluded that for the strongest cross-section area change (TS4), the dominant flow pattern resulted dispersed flow, whereas CAF was the major flow pattern in the other configurations (TS2 and TS3).
- Concentrated pressure drop was evaluated by means of the pressure gradient extrapolation technique. Analysis of localized loss coefficient as a function of mixture superficial velocity showed that the values of loss coefficient are almost constant, irrespective of the oil superficial velocity for sudden contraction TS1 and sudden expansion TS2. However, in the case of stronger area ratio change (TS4), a decreasing trend was observed, which is difficult to be explained and needs further investigation.
- An expression to predict phase holdup was suggested, taking into account the influence of core eccentricity caused by buoyancy, particularly, downstream of sudden expansions. The prediction of oil holdup by the proposed model showed better performance over the available phenomenological and mechanistic models in the open literature. The holdup expression was then introduced in a Two-fluid model in order to predict the pressure gradient, resulting in MAPE=9.3 %, which is a significant improvement compared to the existing models. Accordingly, it is worth noting that a proper estimation of oil holdup in horizontal pipe undergoing

abrupt expansion and contraction is necessary to accurately predict the distributed and concentrated pressure drop.

- Further work is recommended to better understand the limitations in the applicability of the pressure gradient extrapolation method to the evaluation of the localized pressure drop across abrupt cross-section area changes, especially as far as the concept of loss coefficient is extended to two-phase flows,

References

Arney, M.S., Bai, R., Guevara, E., Joseph, D.D., Liu, K. (1993). Friction factor and holdup studies for lubricated pipelining- I experiments and correlations. *International Journal of Multiphase Flow, 19*, 1061-1076.

Attou, A., Bolle, L. (1997). A new correlation for the two-phase pressure recovery downstream from a sudden enlargement. *Chemical Engineering Technology*, 419-423.

Babakhani Dehkordi, P., Azdarpour, A., Mohammadian, E. (2018). The hydrodynamic behavior of high viscous oil-water flow through horizontal pipe undergoing sudden expansion-CFD study and experimental validation. *Chemical Engineering Research and Design I, 39*, 144-161.

Babakhani Dehkordi, P., Colombo, L.P.M., Guilizzoni, M., Sotgia, G. (2017). CFD simulation with experimental validation of oil-water core-annular flows through Venturi and Nozzle flow meters. *Petroleum Science and Engineering*, *149*, 540-552.

Babakhani Dehkordi, P., Colombo, L.P.M., Guilizzoni, M., Sotgia, G., Cozzi, F. (2017b). Quantitative visualization of oil-water mixture behind sudden expansion by high speed camera. *Physics: Conference Series, 882*.

Balakhrisna, T., Ghosh, S., Das, G,. Das, P.K. (2010). Oil-water flows through sudden contraction and expansion in a horizontal pipe- Phase distribution and pressure drop. *Internation Journal of Multiphase Flow*, 13-24.

Bannwart, A.C., Rodriguez, O.M.H., De Carvalho, C.H.M., Vara, Rosa M.O. (2004). Flow patterns in heavy crude oil-water flow. *Journal of Energy Resources Technology, 126*, 184-189.

Brauner, N. (1998). Liquid-liquid two-phase flow. Heat Exchanger Design Handbook. Begell House, New York (Chapter 2.3.5).

Charles, M.E., Govier, G.T., Hodgson, G. (1961). The horizontal pipeline flow of equal density oil-water mixtures. *The Canadian Journal of Chemical Engineering, 1*, 27-36.

Chen, I.Y., Liu, C.C., Chien, K.H., Wang, C.C. (2007). Two-phase flow characteristics across sudden expansion in small rectangular channels. *Experimental Thermal and Fluid Science, 32*, 696-706.

Chen, I.Y., Tseng, C.Y., Lin, Y.T., Wang, C.C. (2009). Two-phase flow pressure change subject to sudden contraction in small rectangular channels. *International Journal of Multiphase Flow, 35*, 297-306.

Chisholm, D. (1983). *Two-phase flow in pipelines and heat exchangers*. Godwin, London. pp. 175-192.

Colombo, L.P.M., Guilizzoni, M., Sotgia, G., Babakhani Dehkordi, P., Lucchini, A. (2017). Water holdup estimation from pressure drop measurements in oil-water two-phase flows by means of the two-fluid model. *Physics: Conference Series, 923*.

Colombo, L.P.M., Guilizzoni, M., Sotgia, G., Marzorati, D. (2015). Infulence of sudden contarctions on in sity volume fractions for oil-water flows in horizontal pipes. *Heat and Fluid Flow, 53*, 91-97.

Colombo, L.P.M., Guilizzoni, M., Sotgia, G.M. (2012). Characterization of the critical transition from annular to wavy-stratified flow for oil-water mixtures in horizontal pipes. *Experiments in fluids, 53*, 1617-1625.

Grassi, B., Strazza, P., Poesio, P. (2008). Experimental validation of theoretical models in two-phase high-viscosity ratio liquid-liquid flows in horizontal and slightly inclined pipes. *International Journal of Multiphase Flow, 34*, 950-965.

Hwang, C-Y. J., Pal, R. (1997). Flow of two-phase oil/water mixtures through sudden expansions and contractions. *Chemical Engineering*, 157-163.

Kaushik, V.V.R., Ghosh, S., Das. G,. Das. P.K. (2012). CFD simulation of core annular flow through sudden contraction and expansion. *Petroleum Science and Engineering, 86*, 153-164.

Loh, W.L., Premanadhan, V.K. (2016). Experimental investigation of viscous oil-water flows in pipeline. *Journal of Petroleum Science and Engineering, 147*, 87-97.

McCabe, W.L., Smith, J.C., Harriott, P. (1993). *Unit Operations of Chemical Engineering.* New York: McGraw-Hill.

Oliemans, R.V.A., Ooms.G., Wu, H., Duijvestjn, A. (1987). Core-annular oil/water flow:The turbulent-lubricatinf-film model and measurements in a 5cm pipe loop. *International Jurnal of Multiphase Flow, 13*, 23-31.

Ooms, G., Segal, A., Van Der Wees, A.J., Meerhoff, R., Oliemans, R.V.A. (1984). A theoretical model for core-annular flow of a very viscous oil core and water annulus through a horizontal pipe. *International Journal of Multiphase Flow, 10*, 41-60.

Shi, J. (2015). *A study on high-viscosity oil-water two-phase flow in horizontal pipes. Ph.D thesis.* Cranfield University.

Shi, J., Lao, L., Yeung, H. (2017). Water-lubricated transport of high-viscosity oil in horizontal pipes: The water holdup and pressure gradient. *Int. J. Multiphase flow, 96*, 70-85.

Sotgia, G., Tartarini, P., Stalio, E. (2008). Experimental analysis of flow regimes and pressure drop reduction in oil-water. *International Journal of Multiphase Flow*, 1161-1174.

Ullmann, A., Brauner, N. (2004). Closure relations for the shear stress in two-fluid models for core-annular flow. *Multiphase Science and Technology, 16*, 355-387.

Van Duin, E., Henkes, R., Ooms, G. (2018). Influence of oil viscosity on oil-water core-annular flow through a horizontal pipe. *Petroleum*, 1-7.

Wadle, M. (1989). A new formula for the pressure recovery in an abrupt dissusor. *International Journal of Multiphase Flow*, 241-256.